International Journal of Physics and Mathematical Sciences ISSN: 2277-2111 (Online)
An Online International Journal Available at http://www.cibtech.org/jpms.htm
2012 Vol. 2 (1) January-March, pp.120-130/Prakash et al.
Research Article

PRECIPITABLE WATER VAPOUR AT SANTACRUZ AIRPORT MUMBAI FROM RADIOSONDE MEASUREMENTS: A STUDY

***Satish Prakash[1], R.K. Giri[2] and Adesh[1]**
[1]Department of Physics, Meerut College Meerut, Uttar Pradesh –UP-250001
[2]India Meteorological Department, Lodi Road, New Delhi-110003.
**Author for Correspondence*

ABSTRACT
A study of 11 years (1995-2005) Precipitable Water (PW) derived from radiosonde data of Santacruz airport (19.7 $^{\circ}$N, 72.51 $^{\circ}$E) Mumbai for both 0000 and 1200 UTC has been carried out. The time series of PW and its deviation from annual mean also brought out for all the years. Both dry and moist years in both monsoon and post monsoon season shows almost increasing trend of PW for all the years except the year 1996 and 2000. It indicates that local modification of weather systems either sea bridge or entrainment of dry or moist air also play an important role in rainfall. There is no significant correlation between rainfall and PW brought out from the above study.

Key Words: *Precipitable Water, Instability, Convection, Rainfall And Universal Time Coordinate (UTC)*

INTRODUCTION

India Meteorological Department (IMD) presently upper air observational netwok consists of 39 radiosonde twice a day (0000 & 1200 UTC) daily for all over the country. Global radiosonde network is shown in Figure 1. The radiosonde contains instruments capable of making direct in-situ measurements of air temperature, humidity and pressure with height, typically to altitudes of approximately 30 km. These observed data are transmitted immediately to the ground station by a radio transmitter located within the instrument package. The ascent of a radiosonde provides an indirect measure of the wind speed and direction at various levels throughout the troposphere. There are several limitations of the radiosonde data incase of heavy precipitation or severe thunderstorms. Typical vertical ascent rates range from 5 to 10ms^{-1} giving ascent times between 1 and 2 hours. Pressure measurements are not reported directly, but are used to determine geopotential heights. The statistics of spatial and temporal atmospheric variations of radiosonde observations from other observations for synoptic applications is given by Kitchen (1989)**.** In his study he explained that the radiosonde observations of the site location are typically displaced by several tens of kilometers horizontally from the observation point. Bruce *et al.,* (1977) utilized radiosonde data to estimate collocation errors for radiosonde/satellite temperature sounding comparisons and noted the paucity of readily available variability statistics the collocate errors. Studies (Zipser *et al.,* 1998) have also shown that sonde humidity measurements tend to exhibit a dry bias at relative humidities close to saturation (100%), so that corrections will often be applied to reported humidities at the upper end of the scale. These ingredients associated with deep convection are the synoptic scale, which has to produce the favourable environment, and the mesoscale, which provides the lifting mechanisms for low-level parcels (Doswell, 1987). Although convection develops in environments with large spatial and temporal variability (Brooks *et al*., 1994), ingredients on the synoptic scale can be evaluated from operational gridded numerical analyses or forecasts. Known favourable mechanisms are upward vertical motion, water-vapour convergence at low levels and potential or latent instability (Doswell, 1987; McNulty, 1995). The area where these positive mechanisms overlap can be considered as favourable for convective development (Ramis *et al*., 1994). Robert *et al.,* (2007) studied that the global deep convection because of enhanced global radiative forcing is associated with elevated greenhouse gas concentrations. Conditional symmetric instability in moist baroclinic atmosphere using gravitational and centrifugal parameters in slantwise direction is determined by atmospheric soundings along a surface of constant angular momentum (Emanuel, KA 1983b). Emanuel, KA 1983a, studied moist symmetric instability under the assumptions that the Froude number is small and the mixing is small**.** Emanuel, KA 1979**,**

shows that circulations resulting from symmetric instability of shear flows have fundamentally mesoscale character and ambient rotation and ageostophic advection is necessary for instability.

Water vapour plays an important role in the transfer of energy and moisture to the atmosphere. The Precipitable Water (PW) is the vertically integrated total mass of water vapor per unit area for a column of atmosphere. Determination of total precipitable water content of the atmosphere column provides an idea of the possible amount of rain that may be expected from the overlying air if conditions become favorable for precipitation of moisture**.**

Information of precipitable water vapour is very important and critical variable for climate studies and significantly contributed to the green house effect (Soden and Bretherton, 1993). Its temporal and seasonal variation is very important to understand the energy budget of the atmosphere over the area. The uneven distribution of water vapour is even more pronounced in the vertical direction. Earlier studies (Kiehl et. al, 1992) have shown the importance of vertical distribution of water vapour for the quantitative definition of the infrared radiation emitted by the atmosphere, as well as for the assessment of the seasonal variations of the precipitable water. The knowledge of its distribution is therefore important to better initialize the constraints of the mesoscale numerical model. The vertical distribution of precipitable water in tropics and extratropical regions are different. In the extratropical regions, the maximum precipitable water vapor is usually found near 700 mb. The study by Banerji et al. (1967) suggests that this is true for the monsoon region also. A numerical method **(**Cartalis et. al, 1997) use radiosonde data to estimate the precipitable water based on temperature and humidity, which shows good agreement with TIROS Operational Vertical Sounder (TOVS) satellite data.

The use of satellite for precipitable water is essential because the ground stations are sparse and over ocean stations are nearly non-existent. To establish resemblance with remotely sensed precipitable water with actual observations a better algorithmic approach is required. In this direction, special sensor for microwave imager (SSM/I) integrated water vapour over the Indian seas shows close proximity with the radiosonde derived precipitable water (Mahajan, 2001).

Convection triggering:

The information obtained from radiosonde observations is utilized in many ways to monitor or diagnose the convective activities in the atmosphere. Various thermodynamic parameters being derived from in-situ radiosonde measurements have been used for convection triggering. In this direction, Weisman, M. and Klemp, J (1982, 1984) studied the Bulk Richardson number (Equation 1) dependencies for severe convective systems and $R_{ig} > 35$ is supportive for multi-cell environment and associated with severe convection.

$$R_{ig} = \frac{2CAPE}{\left(\frac{\partial \bar{V}}{\partial z}\right)^2} \qquad \textbf{(1)}$$

The vertical shear (Eq 2) associated with the horizontal temperature gradient is shown below. The horizontal temperature gradient is very useful in spreading the convective activity over the area.

$$\frac{\partial V}{\partial Z} \cong \frac{g}{fT} K \times \nabla T \qquad \textbf{(2)}$$

Where f is the Coriolis parameter and g is the gravitational acceleration, owing to projected weakening of the horizontal (nominally, equator to pole) gradient of temperature (∇T **).** Severe thunderstorms occur most readily when CAPE and vertical wind shear both are large in a local environment. Hence, one possible outcome from the increased CAPE and decreased shear expected under anthropogenic climate change is the predominance of less organized thunderstorms, still capable of

extreme rainfall but generally nonsevere. Other wave research by Scorer (1949) theorized that mountain waves were a function of atmospheric stability and vertical wind shear according to the equation (3)

$$l^2 = \frac{N^2}{u_0^2} - \frac{1}{u_0}\frac{d^2u_0}{dz^2} \qquad \textbf{(3)}$$

In this similar sequence precipitable water vapor is also a derived product from upper air sounding data. The availability of the derived products depends on the upper air sounding network in which very little number of stations is working and frequency also twice a day (0000 & 1200 UTC). Due to the limited availability, affected by weather, maintenance and expensiveness involved these observations are very crucial. Data obtained through satellite with proper validation can also be used by several researches all over the world. Jewett and Mecikalski (2010) estimated momentum flux using geostationary satellite. Mecikalski and Bedka (2006) use day time Geostationary Operational Environmental Satellite (GOES) for forecasting the initiation of cumulus convection.

MATERIAL AND METHODS

Radiosondes, instrument packages that are carried aloft by balloons launched at hundreds of locations around the world twice a day, measure vertical variations in air temperature, pressure, and humidity up to an altitude of about 30,000 m (100,000 ft). (When tracked for wind information, they are termed radiosondes) A humidity measure, called mixing ratio, is routinely calculated from these data. Mixing ratio is the mass of water vapor (in grams) per mass (kilogram) of dry air. The amount of water vapor in air can be determined from radiosonde data.

The radiosonde data used in the study have been collected from Regional Meteorological Centre, Mumbai. The value of PW can be computed by integrating specific humidity (q) for the whole atmospheric height. This is given in equation (1)

$$PW = {}^{1}\!\!\diagup\!\!{}_{g}\int_{0}^{Ps} q\,dp \qquad (1)$$

The above integral can be evaluated using the trapezoidal rule.

Or

$$PW = {}^{1}\!\!\diagup\!\!{}_{2g}\sum_{i=1}^{n-1}(q_i + q_{i+1})(p_i - p_{i+1}) \qquad (2)$$

Where, q is the specific humidity and p_s is the surface pressure in hPa. The relationship between q and mixing ratio (α) is given below in equation (3). The value of α is again related to the saturation and actual vapour pressure as shown below in equation (4) and (5) respectively. The saturation vapour pressure is related to the air temperature (T) which in $^{\circ}$C by an empirical formula given by Tetens's (Tetens, 1930). Tetens's formula is given below in equation (6).

$$q = \frac{a}{1+a} \qquad (3)$$

$$a = \varepsilon \frac{e}{p - e} \quad (4)$$

Where, ε = 0.622

$$e = e_s \times rh \quad (5)$$

$$e_s = 6.11 \times 10^{\frac{aT}{T+b}} \quad (6)$$

Where, a =7.45 and b= 235 are constants. On the basis of relative humidity and air temperature at different layers in the atmosphere the values of specific humidity is calculated which then sum up to the top of atmosphere. There is uncertainty about the upper limit of integration in equation (1). As we reach up to 10 hPa then the amount of water vapour is low and the instrument for humidity measurement (hygrister) are not practically reliable at temperature below -40 °C. Due to these reasons, generally we take the upper level up to 200 hPa (Elliot and Gaffen, 1991). The drought or moist years or season given in Table 1 & 2 (a-e) is decided as per the criteria of India Meteorological Department.

Table 1: Seasonal and annual PW with rainfall

Season Year	1995	1996	1997	1998	1999	2000	2001	2002	2003	2004	2005
Winter rain (Dec-Feb)	N	D	NR	NR	NR	NR	N	NR	E	NR	S
Winter mean PW in mm	41.75	35.03	40.54	40.16	36.30	30.70	38.26	36.98	44.80	40.80	37.80
Pre-mon rain (March-May)	NR	NR	NR	S	E	E	E	S	NR	E	S
Pre-mon mean PW in mm	69.04	62.42	60.03	66.75	65.16	57.96	61.26	64.15	64.04	63.98	49.16
Monsoon rain (June-Sept)	N	N	N	N	N	N	N	N	N	N	N
Monsoon mean PW in mm	112.43	117.20	120.71	129.44	129.05	110.77	116.73	115.65	130.15	114.12	100.17
Post-mon rain (Oct-Nov)	N	N	NR	D	E	E	E	D	N	E	D
Post-Mon mean PW in mm	73.90	66.43	63.44	84.95	79.76	56.40	66.39	58.31	77.97	65.89	54.88
Annual rain (Jan-Dec)	D	N	D	D	N	N	N	D	N	N	D
Annual mean PW in mm	77.49	74.50	75.95	84.03	81.67	68.49	74.86	73.55	83.59	75.21	64.28

Where, N=Normal rainfall, D=Deficient rainfall, NR=No rainfall S= Scanty rainfall and E= Excess rainfall

RESULTS AND DISCUSSIONS

11 year data (1995-2005) series of upper air radio sounding data for both 0000 and 1200 UTC for each season (Winter, Pre-Monsoon, Monsoon and Post –Monsoon) is shown in Figs (1-4) for Santacruz airport (19.7 $^{\circ}$N, 72.51 $^{\circ}$E) Mumbai . The trend in all the seasons is not regular which is quite obvious because every year the intensity and approach of the weather systems is different and moisture availability is modified by the local effects.

Table 2(a): Mean (μ), standard deviation (σ) and coefficient of variation (α) of PW for winter season at the station Santacruz airport Mumbai.

Season	Year		1995 (N)	1996 (D)	1997 (NR)	1998 (NR)	1999 (NR)	2000 (NR)	2001 (N)	2002 (NR)	2003 (E)	2004 (NR)	2005 (S)
Winter	00:00 UTC	μ	21.03	17.85	19.69	19.49	18.85	15.22	19.55	19.08	22.31	20.63	19.79
		σ	8.04	9.41	8.60	9.48	8.26	8.96	11.44	7.28	9.52	8.83	8.34
		α	0.38	0.52	0.44	0.49	0.44	0.59	0.59	0.38	0.43	0.43	0.42
Winter	12:00 UTC	μ	20.64	17.25	20.03	20.48	17.80	15.39	18.81	17.79	22.70	20.11	18.03
		σ	8.03	8.49	9.43	9.80	8.00	9.14	7.84	6.88	8.51	9.35	7.94
		α	0.41	0.49	0.47	0.48	0.45	0.59	0.42	0.38	0.38	0.46	0.44

Where, N=Normal rainfall, D=Deficient rainfall, NR=No rainfall and S= Scanty rainfall

Table 2(b): Mean (μ), standard deviation (σ) and coefficient of variation (α) of PW for pre-monsoon season at the station Santacruz airport Mumbai.

Season	Year		1995 (NR)	1996 (NR)	1997 (NR)	1998 (S)	1999 (E)	2000 (E)	2001 (E)	2002 (S)	2003 (NR)	2004 (E)	2005 (S)
Pre-monsoon	00:00 UTC	μ	36.16	28.89	31.41	34.79	33.01	29.15	32.65	32.67	33.77	32.61	25.10
		σ	25.33	13.07	9.23	12.72	14.85	13.28	14.2	11.92	14.81	14.00	11.01
		α	0.70	0.45	0.29	0.37	0.45	0.46	0.43	0.36	0.44	0.43	0.44
Pre-monsoon	12:00 UTC	μ	33.27	25.14	29.60	31.80	32.55	25.29	29.19	31.59	30.35	31.52	22.97
		σ	12.63	12.64	10.11	12.98	15.89	12.68	14.97	11.70	12.79	17.3	11.96
		α	0.37	0.45	0.34	0.41	0.49	0.50	0.51	0.37	0.44	0.55	0.52

Where, N=Normal rainfall, D=Deficient rainfall, NR=No rainfall and S= Scanty rainfall

Table 2(c): Mean (μ), standard deviation (σ) and coefficient of variation (α) of PW for monsoon season at the station Santacruz airport Mumbai.

Season	Year		1995 (N)	1996 (N)	1997 (N)	1998 (N)	1999 (N)	2000 (N)	2001 (N)	2002 (N)	2003 (N)	2004 (N)	2005 (N)
Monsoon	00:00 UTC	μ	55.84	58.38	59.83	64.32	63.59	57.17	53.86	57.06	62.97	56.35	58.13
		σ	11.68	8.80	12.17	11.00	10.99	13.50	12.65	13.53	12.21	13.11	8.97
		α	0.20	0.15	0.20	0.17	0.09	0.24	0.23	0.24	0.19	0.23	0.18
Monsoon	12:00 UTC	μ	56.99	58.78	61.78	65.11	65.62	54.89	62.77	58.53	67.48	58.09	58.10
		σ	12.03	11.75	13.50	13.73	12.92	16.18	14.56	14.08	14.38	15.21	11.74
		α	0.21	0.19	0.22	0.21	0.20	0.29	0.23	0.24	0.21	0.26	0.23

Where, N= Normal rainfall

Table 2(d): Mean (μ), standard deviation (σ) and coefficient of variation (α) of PW for post-monsoon season at the station Santacruz airport Mumbai.

Season	Year		1995 (N)	1996 (N)	1997 (NR)	1998 (D)	1999 (E)	2000 (E)	2001 (E)	2002 (D)	2003 (N)	2004 (E)	2005 (D)
Post-monsoon	00:00 UTC	μ	37.58	32.43	34.30	41.50	43.27	24.67	31.69	28.91	40.43	32.93	28.59
		σ	19.09	14.72	10.36	18.14	20.44	12.88	17.58	14.42	14.15	13.38	12.27
		α	0.50	0.46	0.30	0.43	0.47	0.52	0.55	0.49	0.42	0.41	0.43
Post-monsoon	12:00 UTC	μ	36.53	33.85	32.95	43.44	41.22	26.85	33.08	29.32	33.52	32.58	28.26
		σ	16.08	16.49	12.00	21.34	23.28	15.95	17.50	12.96	17.15	14.71	12.39
		α	0.45	0.49	0.36	0.49	0.56	0.59	0.52	0.44	0.45	0.45	0.43

Where, N=Normal rainfall, D=Deficient rainfall, NR=No rainfall and S= Scanty rainfall

Table 2(e): Mean (μ), standard deviation (σ) and coefficient of variation (α) of PW for annual at the station Santacruz airport Mumbai.

Season Year			1995 (D)	1996 (N)	1997 (N)	1998 (N)	1999 (D)	2000 (N)	2001 (N)	2002 (D)	2003 (N)	2004 (N)	2005 (E)
Annual	00:00 UTC	μ	39.13	39.93	38.14	42.32	41.72	34.70	39.6	36.89	41.94	37.79	32.84
		σ	21.40	19.98	19.00	21.5	22.26	21.22	19.19	19.39	20.73	18.94	16.14
		α	0.55	0.54	0.49	0.50	0.53	0.61	0.52	0.52	0.51	0.5	0.49
Annual	12:00 UTC	μ	28.24	36.28	37.42	41.63	40.75	31.69	38.03	36.73	41.87	37.94	31.54
		σ	18.72	21.01	20.27	22.8	23.99	20.90	22.58	20.03	22.75	21.03	17.36
		α	0.49	0.58	0.54	0.54	0.58	0.66	0.59	0.54	0.54	0.55	0.56

Where, N=Normal rainfall, D=Deficient rainfall, NR=No rainfall and S= Scanty rainfall

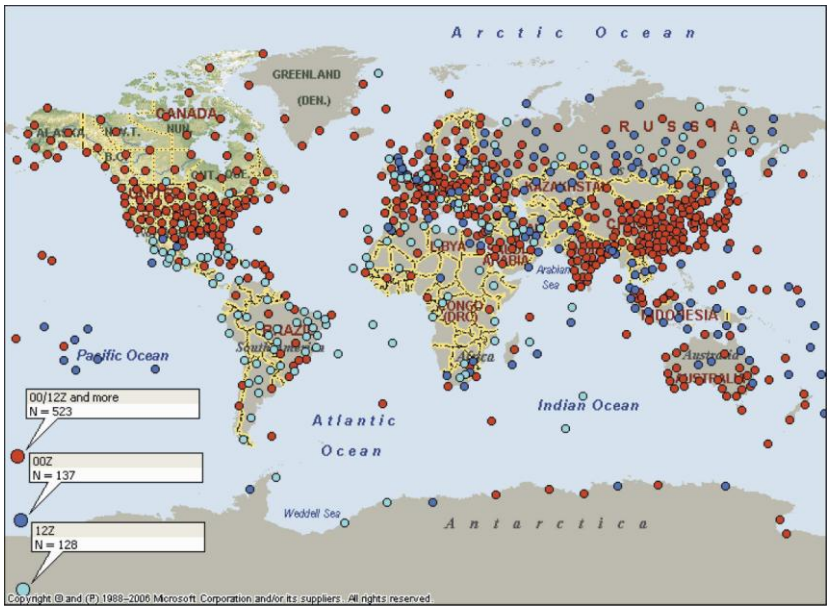

Figure 1: Radiosonde observation Network [Source: Wang J and Jhang L (2008) , Journal of climate]

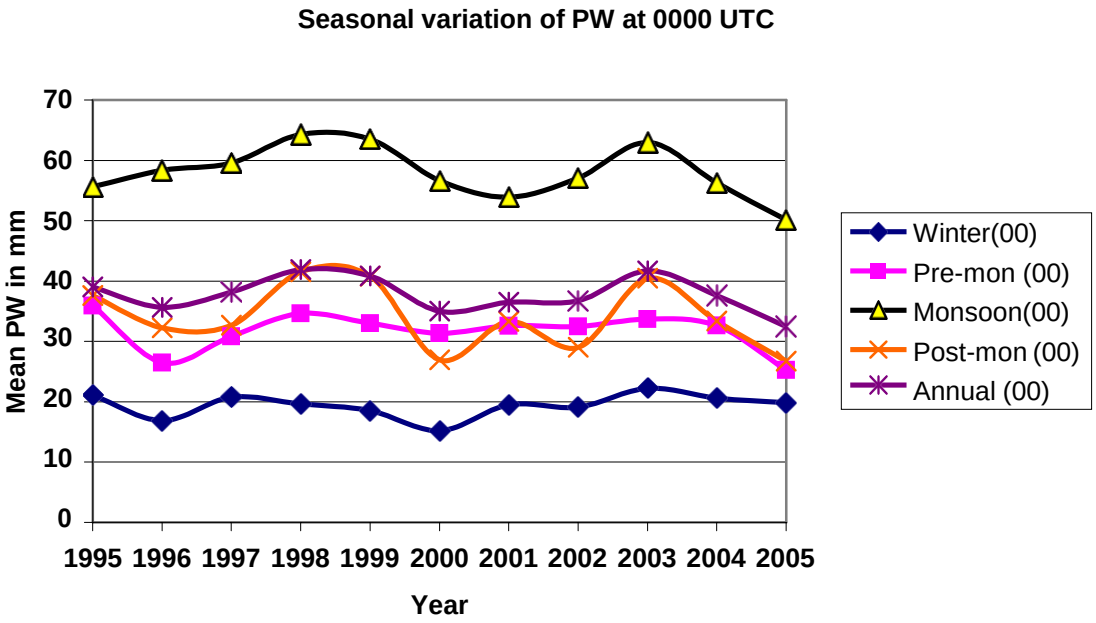

Figure 2: Seasonal variation of PW at 0000 UTC

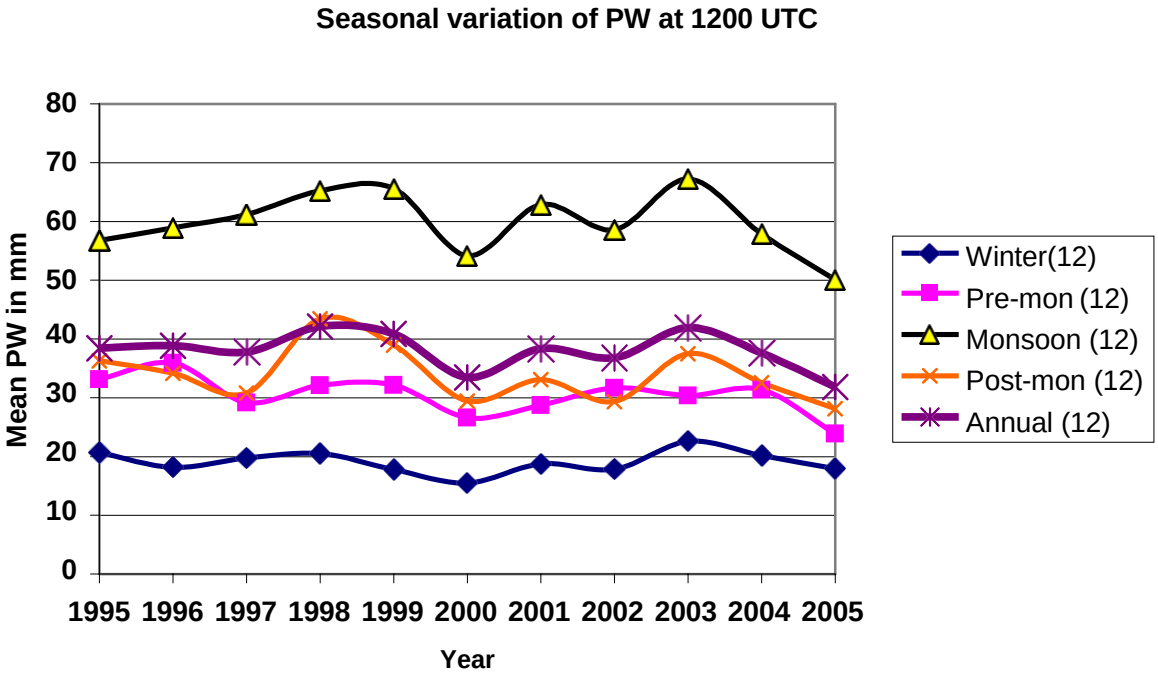

Figure 3: Seasonal variation of PW at 1200 UTC

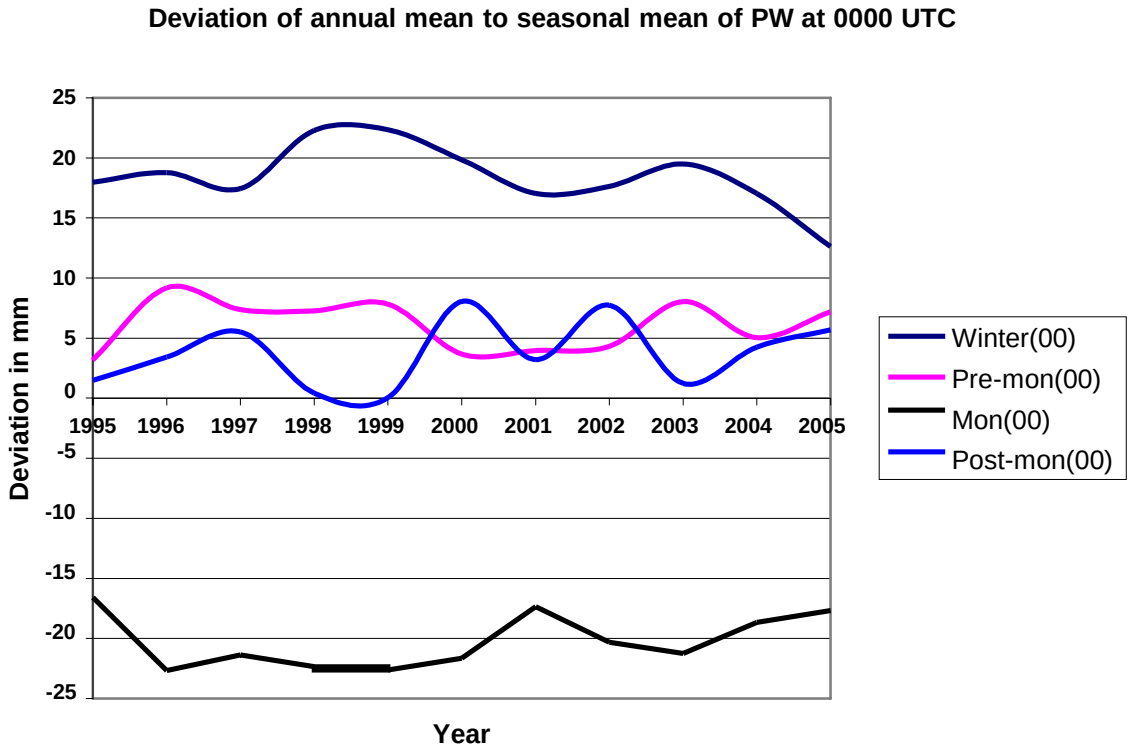

Figure 4: Deviation of annual mean to seasonal (annual-seasonal) of PW at 0000 UTC

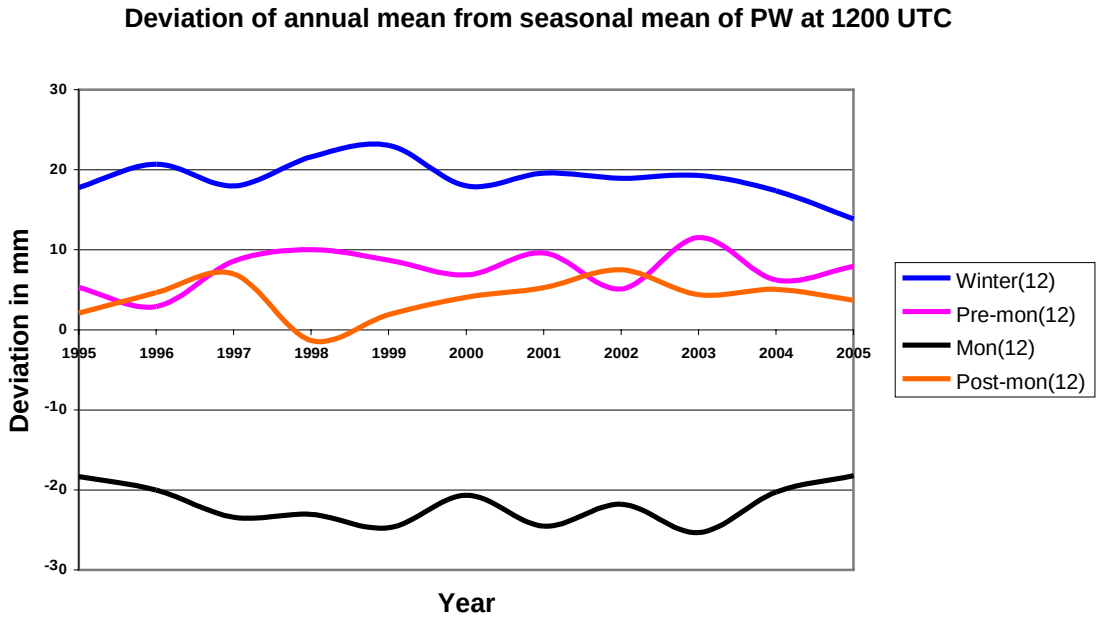

Figure 5: Deviation of annual mean to seasonal (annual-seasonal) of PW at 1200 UTC

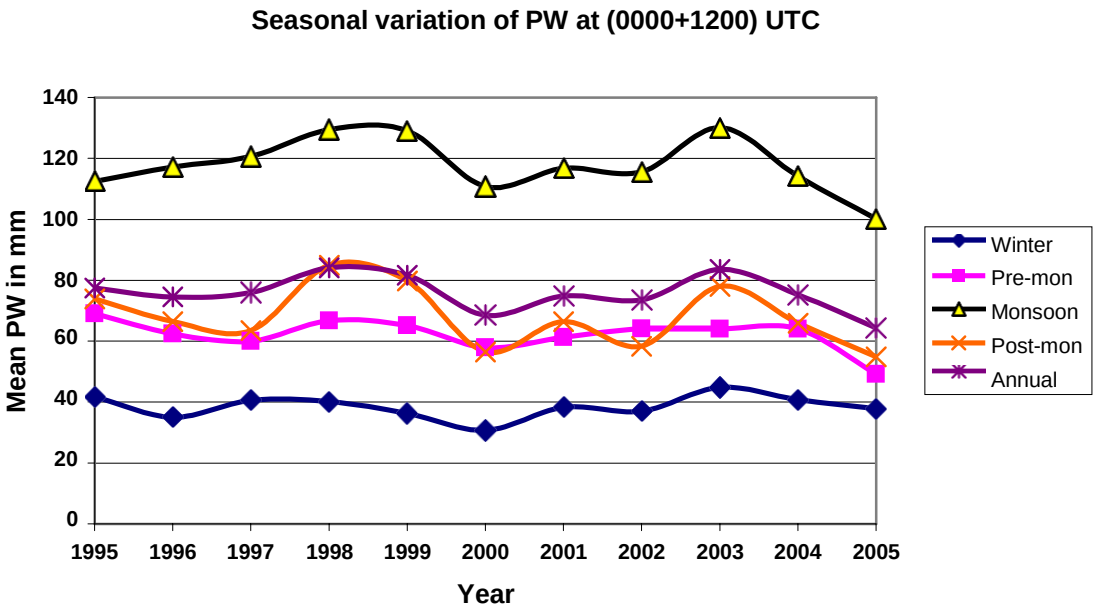

Figure 6: Deviation of annual mean to seasonal (annual-seasonal) of PW at 1200 UTC

Diurnal variation of water vapor and convective activity are locally modified of the area those are near to the coast. Basic synoptic scale systems are thermally induced system and Sea Bridge which locally modifies the moisture availability. The water vapor increases in the mixing layer can be associated with the "extended sea breeze" from the morning to the evening and due to both evaporation from surface and moisture convergence**.** It has been observed from Fig.2 that the yearly mean of PW at 0000 UTC increases gradually in the years 1996 to 1998 and the year 2000-2003 .The similar trend is observed for 1200 UTC which is shown in Fig.3 with lesser smoothness as compared to 0000 UTC for all the season. This may be due to the stability of the atmosphere decreases in the evening as a result of the increase of water vapor in the lower layer, which contribute to the evening convective maxima over the semi-basin (Iwasaki and Miki 2002). This monitoring and analysis is important to issue the timely forecast or warning related to the extreme weather events like heavy rainfall warning, floods etc.

The coefficient of variation (α) in PW for both 0000 and 1200 UTC are lesser for monsoon season in comparison to the annual and other seasons. This may be due to that the air is almost saturated and no large changes have been contributed significantly. This is seen clearly in statistical analysis given in Table 2 (a-e). Other possible reason may that the data may not yield reliable value at high levels in bed weather conditions. So, any major change is filtered out from the observed data. In other words, the smaller perturbations are automatically filtered out in the mean trends of PW. The standard deviations (σ) for winter season are smaller in comparison to the annual and other seasons Table 2(a-e). The mean values (μ) for monsoon season in both 00:00 and 12:00 UTC are higher in comparison to other seasons. This is due to the availability of more moisture in this season.

PW is not the direct index of rainfall activity, unless a condition becomes favorable for precipitation of moisture. The year 2005 is excess rainfall year due to monsoon rainfall and rest three seasons in this year are having very less rainfall. Another possibility is that the convective systems are favoured by situations having distinct synoptic characteristics: upward large-scale velocity, convergence of water vapour at low levels, and instability as well as sub-synoptic (mesoscale) mechanisms for initiating convection (Doswell, 1987). An important challenge is the determination of the likelihood of

convective development occurrence, its related strength and associated meteorological phenomena, on the basis of the synoptic-scale meteorological conditions (Tudurì and Ramis, 1997).

Known problems of radiosonde data

Wang J and Zhang L (2008) shows that the radiosonde data have long-term temporal inhomogeneity, and diurnal sampling errors of once- and twice-daily radiosonde data. The dry bias in Vaisala radiosondes has larger magnitudes during the day than at night, especially for RS90 and RS92, with a day–night difference of 5%–7%. Diurnal sampling errors of twice-daily radiosonde data are generally within 2%, but can be as much as 10%–15% for the once-daily soundings. Drifting of the balloon in the air and limited vertical extent during heavy rainy days and sensor limitations in very cold and high temperature areas affects the accuracies of the upper air observations. The above said inherent as well as instrumental problems are also remained during the analysis.

CONCLUSION

Upper air sounding through balloons is quite old technique to probe the atmosphere. The thermal and moisture distribution over the station twice a day (0000 & 1200 UTC) at different layers in the atmosphere may be known within the inherent limits of the accuracy. The information obtained through sounding is very useful in monitoring the convection and other associated weather phenomenon either by data or derived stability parameters. In this work one derived product of precipitable water of the entire column is utilized for the Santacruz station of Mumbai. Mumabi is a coastal station and their climate or day to weather is very much affected by the local events. It has been seen that 0000 UTC precipitable water vapour trend over the years (1995-2005) is quite smooth as compared to 1200 UTC. The possible region may be the localized sea bridge to broken the latent instability and support vertical motion. The statistical analysis mean or standard deviations are quite regular for winter and monsoon seasons as compared to pre-monsoon and post-monsoon seasons. This is possibly due to less frequent variations of moisture and temperature as compared to pre and post monsoon seasons. Because during monsson season the atmosphere is frequently becomes saturated with moisture and in winter moisture content is very less and prevails almost the same over the month or winter season. Studies above indicates that the regional models after assimilating the above sounding data may improve the temperature and moisture fields initial fields and in turn overall forecasting.

ACKNOWLEDGEMENTS

The authors are very grateful to DGM, IMD for providing the data. The contributions of the supporting staff of Meerut College duly acknowledged.

REFERENCES

Banerji S, Rao DVLN, Julka ML, and Anand CM (1967). Some Further Results of Investigations on Quantitative Precipitation Forecasting Over Selected Areas in North India**,** *Indian Journal of Meteorology and Geophysics***,** *India Meteorological Department* **18**(4) 465-472.

Brooks HE, Doswell III CA & Cooper J (1994). On the environments of tornadic and nontornadic environments. *WeatherForecasting,* **9 (3)** 606–618.

Bruce RE, Duncan L D and Pierluissi J H (1977). Experimental study and relationship between radiosonde temperature and satellite derived temperatures, *Monthly Weather Review* **105**(4) 493-496.

Cartalis C and Chrysoulakis N (1997). Estimation of Precipitable water in Greece on the basis of radiosondes and satellite data, *Toxicological and Environmental Chemistry* **58**(1)163-171.

Doswell III CA (1987). The distinction between large-scale and mesoscale contribution to severe convection: a case study example. *Weather Forecasting,* **2**(1) 3–16.

Emanuel KA (1979). Inertial instability and mesoscale convective systems. Part I: Linear theory of inertial instability in rotating viscous fluids, *Journal of Atmospheric Sciences* **38**(12) 2425-2449.

Emanuel K.A. (1983a). The Lagrangian parcel dynamics of moist symmetric instability. *Journal of Atmospheric Sciences* **40** 2368-2376.
Emanuel, KA (1983b). On assessing local conditional symmetric instability from atmospheric soundings. *Monthly Weather Review* 111**(10)** 2016-2033.
Elliott WP and Gaffen DJ (1991). On the utility of radiosonde humidity archives for climate studies, Bulletin of American. Meteorological Society **72**(10) 1507-1520.
Iwasaki and Miki (2002). Diurnal variation of convective activity and precipitable water over the "semi-basin" Preliminary study on the mechanismresponsible for the evening convective activity maximum *Journal of Meteorological Society Japan* **80**(3) 439-450**.**
Jewett CP and Mecikalski JR (2010). Estimating convective momentum fluxes using geostationary satellite data. *Journal of Geophysical Research Atmosphere*, 115(1) D14.
Kiehl JT and Briegleb BP (1992). A comparison of the observed and calculated clear sky greenhouse effect: Implications for climate studies. *Journal of Geophysical Research* **97 (D9)**10037-10049.
Kitchen M (1989). Representativeness errors of radiosonde observations, *Quaterly Journal of Royal Meteorological Society***, 115 (487)** 673-700
McNulty, R. P. (1995). Severe and convective weather: a central region forecasting challenge. *Weather Forecasting*, **10 (1)** 187–202.
Mecikalski, JR and Bedka, KM (2006). Forecasting Convective Initiation by Monitoring the Evolution of Moving Cumulus in Daytime GOES Imagery**.** *Monthly Weather Review* **134**(1) 49-78**.**
Ramis, C., Arús, J., López, J. L. & Mestre, A. (1997). Two cases of severe weather in Catalonia (Spain). An observational study. *Meteorooical Applications* **4 (1)** 207–217.
Robert J. Trapp, Noah S. Diffenbaugh , Harold E. Brooks , Michael E. Baldwin, Eric D. Robinson, and Jeremy S. Pal (2007). Changes in severe thunderstorm environment frequency during the 21st century caused by anthropogenically enhanced global radiative forcing**.** *Proceedings of the national academy of sciences, USA* **104 (50)** 19719-19723
Scorer R. (1949). Theory of waves in the lee of mountains**.** *Quarterly Journal of Royal Meteorological Society*, **75 (1)** 41-56.
Soden BJ and Bretherton FP (1993). Upper tropospheric relative humidity from the GOES 6.7 µm channel: Method and climatology for July 1987, *Journal of Geophysical Research***, 98 (D9)** 16669-16688.
Tetens O (1930). Uber einige meteorologische begriffe Z ***Geophysics*** 6 (2) 297-309**.**
Tudurì E and Ramis C (1997). The environments of significant convective events in the Western Mediterranean. *Weather Forecasting* 12 (2) 294–306.
Weisman M and Klemp, J (1982). The dependence of numerically simulated convective storms on vertical wind shear and buoyancy. *Monthly Weather Review* **110 (6)** 504–20.
Weisman M & Klemp, J. (1984). The structure and classification of numerically simulated convective storms in directionally varying wind shears. *Monthly Weather Review* **112 (12)** 2479–98
Wang J and Zhang L (2008). Systematic Errors in Global Radiosonde Precipitable Water Data from Comparisons with Ground-Based GPS Measurements, *Journal of Climate* 21 (10), 2218-2238.
Zipser E and Johnson R (1998). Systematic errors in radiosonde humidities: a global problem? Tenth symposium on Meteorological Observations and Instrumentation, *Phoenix Arizona* **72-73.**